EUKARYOTIC CELL, Mar. 2007, p. 454–464 Vol. 6, No. 3
1535-9778/07/$08.00+0 doi:10.1128/EC.00283-06

De Novo Sphingolipid Synthesis Is Essential for Viability, but Not for Transport of Glycosylphosphatidylinositol-Anchored Proteins, in African Trypanosomes[▽]

Shaheen S. Sutterwala,[1] Caleb H. Creswell,[2] Sumana Sanyal,[3] Anant K. Menon,[3] and James D. Bangs[1]*

Department of Medical Microbiology and Immunology[1] and Department of Biochemistry,[2] University of Wisconsin School of Medicine and Public Health, Madison, Wisconsin 53706, and Department of Biochemistry, Weill Medical College of Cornell University, New York, New York 10021[3]

Received 5 September 2006/Accepted 20 December 2006

De novo sphingolipid synthesis is required for the exit of glycosylphosphatidylinositol (GPI)-anchored membrane proteins from the endoplasmic reticulum in yeast. Using a pharmacological approach, we test the generality of this phenomenon by analyzing the transport of GPI-anchored cargo in widely divergent eukaryotic systems represented by African trypanosomes and HeLa cells. Myriocin, which blocks the first step of sphingolipid synthesis (serine + palmitate → 3-ketodihydrosphingosine), inhibited the growth of cultured bloodstream parasites, and growth was rescued with exogenous 3-ketodihydrosphingosine. Myriocin also blocked metabolic incorporation of [^{3}H]serine into base-resistant sphingolipids. Biochemical analyses indicate that the radiolabeled lipids are not sphingomyelin or inositol phosphorylceramide, suggesting that bloodstream trypanosomes synthesize novel sphingolipids. Inhibition of de novo sphingolipid synthesis with myriocin had no adverse effect on either general secretory trafficking or GPI-dependent trafficking in trypanosomes, and similar results were obtained with HeLa cells. A mild effect on endocytosis was seen for bloodstream trypanosomes after prolonged incubation with myriocin. These results indicate that de novo synthesis of sphingolipids is not a general requirement for secretory trafficking in eukaryotic cells. However, in contrast to the closely related kinetoplastid *Leishmania major*, de novo sphingolipid synthesis is essential for the viability of bloodstream-stage African trypanosomes.

A subset of eukaryotic cell surface proteins is attached to the outer leaflet of the plasma membrane lipid bilayer via glycosylphosphatidylinositol (GPI) anchors. GPI attachment occurs in the endoplasmic reticulum (ER), and GPI anchors can function subsequently in protein sorting within the secretory and endocytic pathways (40). In mammalian cells, GPI anchors influence protein sorting to the apical and basolateral plasma membrane domains of polarized epithelia (12, 39, 55). In *Saccharomyces cerevisiae*, GPI anchor addition is required for efficient ER exit of the GPI-anchored protein Gas1p (20). Furthermore, the GPI anchor plays a role in protein sorting as GPI-anchored proteins are segregated from other secretory proteins and exit the ER in a distinct population of coated vesicles (45). Thus, GPI anchors can function in protein trafficking in both early and late compartments of the secretory pathway in a variety of eukaryotic cells.

African trypanosomes are human and veterinary parasites that belong to the family Kinetoplastida, a phylogenetically ancient group of eukaryotes containing many human pathogens, including South American trypanosomes and members of the genus *Leishmania*. In common with these related protozoa, African trypanosomes have a dense cell surface coat composed of GPI-anchored macromolecules that are essential for survival and pathogenesis within the host (23). The trypanosome life cycle alternates between the midgut of the insect vector (procyclic stage) and the bloodstream of the mammalian host, and trypanosomes have distinct surface proteins at each stage. Variant surface glycoprotein (VSG), the major coat protein of bloodstream-form trypanosomes, is initially synthesized in the ER, where it acquires a GPI anchor, and is then rapidly transported via the Golgi apparatus to the cell surface (4, 6, 22, 24). Our previous studies using VSG reporters lacking a GPI anchor suggest that GPI anchors function as sorting signals at multiple steps in the secretory pathway of bloodstream trypanosomes (7, 41, 60); VSG lacking a GPI anchor shows a delay in ER exit, and upon exit it is mistargeted to the lysosome (60). These findings suggest a requirement for the GPI anchor in export from the ER and also later in the secretory pathway, for targeting to the cell surface.

The mechanisms by which GPI anchors function as sorting signals remain unclear. Unlike transmembrane proteins, GPI-anchored proteins cannot interact directly with cytoplasmic proteins that recognize specific sorting signals. However, the observed association of GPI-anchored proteins with cholesterol and sphingolipid-rich membrane microdomains (3, 13, 57), commonly referred to as lipid rafts, is hypothesized to have functional significance for GPI-dependent protein sorting (34). Lipid rafts in intact cells are thought to correspond operationally to detergent-resistant membranes (DRMs), which are insoluble in cold, non-ionic detergents and are enriched in sterols, sphingolipids, free GPI, and GPI-anchored proteins (13, 31). Consistent with the presence of sphingolipids in DRMs, inhibitors of sphingoid base synthesis, e.g., myriocin, retard the exit of GPI-anchored Gas1p from the ER in yeast

* Corresponding author. Mailing address: Department of Medical Microbiology and Immunology, University of Wisconsin—Madison Medical School, 1300 University Ave., Madison, WI 53706. Phone: (608) 262-3110. Fax: (608) 262-8418. E-mail: jdbangs@wisc.edu.

▽ Published ahead of print on 12 January 2007.

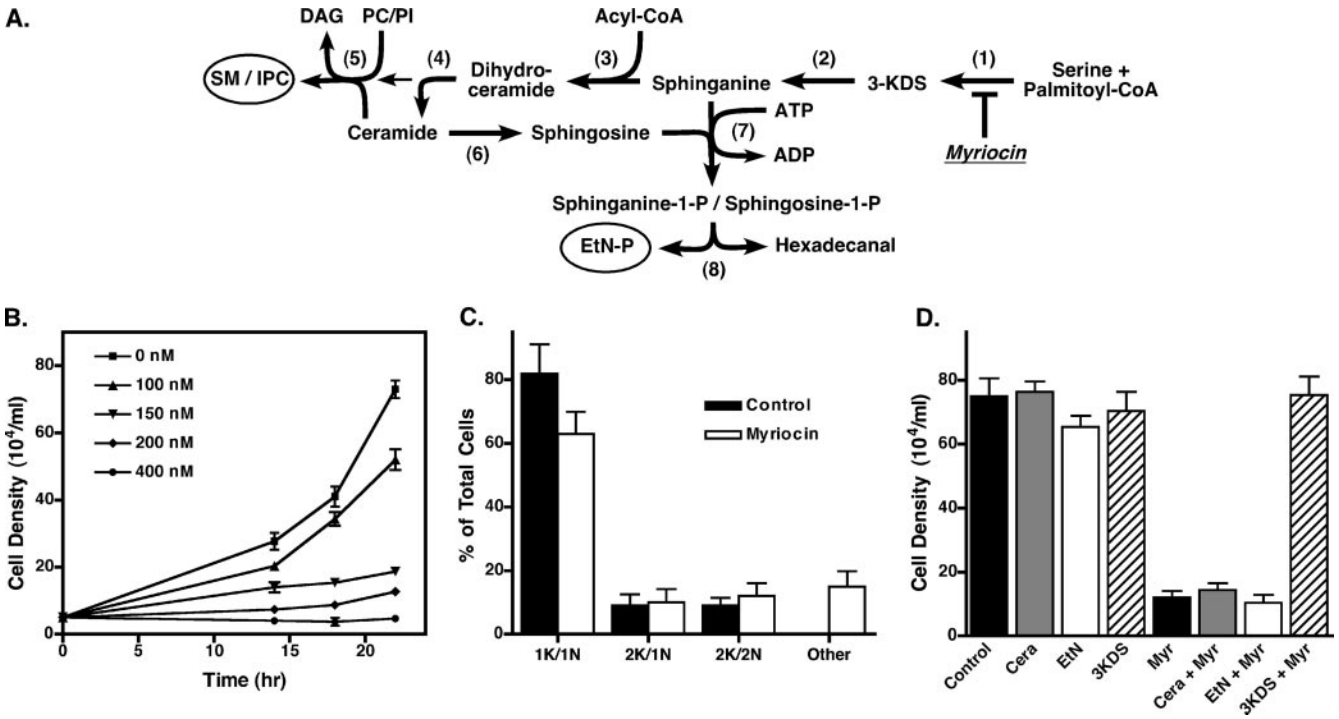

FIG. 1. Cell growth is inhibited by myriocin. (A) The sphingoid lipid pathway. Enzymes are indicated by numbers in parentheses as follows: (1), serine palmitoyltransferase; (2), 3-ketosphingosine reductase; (3), dihydroceramide synthase;(4), dihydroceramide desaturase; (5), "sphingolipid" synthase; (6), ceramidase; (7), sphingosine kinase; (8), sphingosine-1-phosphate lyase. Final end products are sphingomyelin (SM), inositol phosphorylceramide (IPC), and ethanolamine phosphate (EtN-P). Other abbreviations are 3-ketodihydrosphingosine (3-KDS), phosphatidylcholine (PC), phosphatidylinositol (PI), and diacylglycerol (DAG). The site of inhibition by myriocin is indicated. (B) Bloodstream cell cultures were seeded at 1×10^5 cells/ml in the presence of the indicated concentrations of myriocin, and densities were counted at the indicated times. Means ± standard deviations of triplicate cultures were determined. (C) Fixed and permeabilized bloodstream cells were stained with DAPI to reveal the localization of the nucleus and kinetoplast. The numbers of nuclei and kinetoplasts per cell were counted ($n = 100$) for myriocin-treated (200 nM, 18 h) and control cultures. Data are means ± standard deviations from three independent experiments. (D) Bloodstream trypanosomes were seeded at 1×10^5 cells/ml and grown for 18 h in the presence or absence of 200 nM myriocin with additional supplementation with either 2.5 μM 3-KDS, 10 μM ceramide (Cera), or 100 μM ethanolamine (EtN). Values are means ± standard deviations from triplicate cultures.

(59). Furthermore, temperature-sensitive yeast mutants, defective in ceramide and sphingolipid synthesis, also show defects in the trafficking of GPI-anchored molecules, as well as in endocytosis and stress responses (50, 59, 65). These findings have led to the general assumption that ongoing sphingolipid synthesis is required for efficient exit of GPI-anchored proteins from the ER, although this phenomenon has not been validated for eukaryotic cells other than yeast.

The first and rate-limiting step in sphingolipid biosynthesis (Fig. 1A), occurring in the ER, is the condensation of L-serine and palmitoyl coenzyme A (palmitoyl-CoA) into 3-ketodihydrosphingosine (3-KDS), catalyzed by the enzyme serine palmitoyltransferase (SPT). 3-KDS undergoes further modification and is N acylated to generate ceramide, which, following transport to the Golgi apparatus, is converted into higher-order sphingolipids by addition of various polar head groups (29). Plants typically synthesize neutral glycosphingolipids, while mammalian cells produce sphingomyelin, as well as neutral and acidic glycosphingolipids (43). Among the lower eukaryotes *Plasmodium* spp. also make sphingomyelin (28), while many others, including fungi (38), *Toxoplasma gondii* (58), and the kinetoplastids *Leishmania* (35) and *Trypanosoma cruzi* (54), synthesize inositol phosphorylceramide (IPC). Surprisingly, in *Leishmania major*, synthesis of sphingolipids is not necessary for viability or virulence (17, 68), provided the growth medium is supplemented with ethanolamine (67). Due to their close phylogenetic relationship, it has been casually assumed that all kinetoplastids, including African trypanosomes, synthesize IPC (18, 19, 32), and this has recently been confirmed for procyclic-stage *Trypanosoma brucei* (27).

In this study, we investigate these assumptions by using myriocin to block sphingoid base synthesis in bloodstream-stage trypanosomes and mammalian cells. This strategy allows us to directly investigate whether de novo sphingolipid synthesis is required for trypanosome viability and for VSG trafficking. In agreement with previous studies on yeast and mammalian cells (30, 51), and in contrast to *Leishmania*, we find that de novo synthesis of sphingoid base is essential for the viability of African trypanosomes. However, disruption of sphingolipid catabolism has no effect on the trafficking of GPI-anchored-proteins in trypanosomes or in human HeLa cells. Indeed, other than ultimate lethality, the only significant effect we observe in bloodstream trypanosomes is a general depression of endocytosis following prolonged inhibition of sphingoid base synthesis. Finally, metabolic radiolabeling studies with [^{3}H]serine indicate that bloodstream trypanosomes synthesize a novel sphingolipid that is neither IPC, as in *Leishmania*, nor sphingomyelin, as in mammalian cells. Thus, African trypano-

somes differ significantly from related kinetoplastids in the biosynthesis and utilization of sphingolipids.

MATERIALS AND METHODS

Compounds and reagents. Myriocin (Sigma, St. Louis, MO) was prepared as a 1 mg/ml stock solution in methanol. Ethanolamine in liquid form, tunicamycin, brefeldin A (BFA), bovine liver phosphatidylinositol (PI), and bovine brain sphingomyelin were also obtained from Sigma. Both d18:1/18:0 ceramide from Avanti (Alabaster, AL) and 3-KDS from Matreya (Pleasant Gap, PA) were prepared as 10 mM stock solutions in chloroform-methanol (1:1, vol/vol). Glucosylceramide was obtained from Avanti. *Staphylococcus aureus* sphingomyelinase was from Sigma, and *S. aureus* PI-specific phospholipase C (PI-PLC) was a generous gift from Vicky Stevens (Emory University).

Metabolic labeling and analysis of radiolabeled lipids. Cultured procyclic and bloodstream-stage *Trypanosoma brucei brucei* strain Lister 427 parasites were grown and maintained as described in references 2 and 5. Monolayer cultures of HeLa cells were maintained in Dulbecco's modified Eagle medium supplemented with 10% fetal bovine serum (FBS), 100 U/ml penicillin, and 100 μg/ml streptomycin. Bloodstream-stage trypanosomes were harvested at late-log phase (0.5×10^5 to 1×10^5/ml) and resuspended (5×10^7 cells/ml) in TMB medium (48) supplemented with 5% dialyzed fetal calf serum in the presence of myriocin (200 nM) or an equivalent concentration of vehicle. Cells were then metabolically labeled with [^{3}H]serine (20 Ci/mmol; American Radiolabeled Chemicals, Inc., St. Louis, MO) at 50 μCi/ml for 2 to 4 h at 37°C. HeLa cells were preincubated for 20 min in a serine-free medium containing myriocin (62.5 μM) or an equivalent concentration of vehicle before being incubated with 10 μCi/ml [^{3}H]serine for 4 to 8 h. In each case, [^{3}H]serine-labeled lipids were extracted from washed cells in chloroform-methanol-water (CMW; 10:10:3 [vol/vol/vol]). The CMW extract was dried and subjected to *n*-butanol/water partitioning. The organic phase was saponified by drying, resuspension in 0.1 N KOH in methanol, and incubation at 40°C for 1.5 h. The reaction products were neutralized by addition of 20% 1.0 N acetic acid and desalted by *n*-butanol/water partitioning.

For treatment with sphingomyelinase, saponified [^{3}H]serine-labeled lipids were dried with 50 μg sphingomyelin and dissolved in 300 μl of 20 mM Tris-HCl (pH 7.4)–10 mM $MgCl_2$–0.05% (wt/vol) Triton X-100 with or without 1 U of the enzyme. Samples were incubated at 37°C for 2 h, reactions were stopped by addition of 10 μl acetic acid, and lipids were extracted by *n*-butanol/water partitioning. For treatment with PI-PLC, saponified [^{3}H]serine-labeled lipids were dried with 50 μg phosphatidylinositol and dissolved in 100 μl of 50 mM Tris-HCl (pH 7.4)–0.1% deoxycholate with or without the enzyme. Samples were incubated at 37°C for 1 h, reactions were stopped by addition of 10 μl acetic acid, and lipids were extracted by *n*-butanol/water partitioning. Acid methanolysis was adapted from reference 10. Saponified [^{3}H]serine-labeled lipids were dried and suspended in 2 N HCl–80% methanol (1 ml) with ceramide as an internal standard/reactant. Samples in sealed vials were incubated (90°C, 2 h), and fatty methyl esters were then extracted in hexane (1 ml). The remaining aqueous phase was neutralized with 2 N NaOH, and sphingoid bases were extracted in *n*-butanol (1 ml) and dried. All lipid samples were fractionated on Silica 60 plates. Saponified lipids, with or without enzymatic treatment, were resolved in 65:25:4 (vol/vol/vol) CMW. Sphingoid base products of acid methanolysis were resolved in 40:10:1 (vol/vol/vol) chloroform–methanol–2.5 M NH_4OH. The chromatograms were scanned using a Berthold LB2842 thin-layer chromatography (TLC) linear radioactivity analyzer. All radiolabeled lipid species and/or products were identified by comigration of unlabeled internal lipid standards, substrates, or products visualized by iodine staining.

Analysis of protein trafficking in trypanosomes. Pulse-chase metabolic radiolabeling ([^{35}S]methionine-cysteine) of cultured trypanosomes was performed exactly as described in references 2 and 5. For analysis of BiPN secretion, cells were processed into cell and medium fractions and lysed as described previously (5). For analysis of VSG delivery to the surface, cells were hypotonically lysed as described previously (4) to allow conversion of susceptible membrane form VSG to soluble VSG by endogenous GPI-PLC. Briefly, cells were lysed hypotonically (5 min, distilled H_2O containing protease inhibitor cocktail) on ice, the lysate was adjusted to 1× TEN salts (50 mM Tris-HCl [pH 7.5], 5 mM EDTA, 150 mM NaCl), and a further incubation (10 min, 37°C) was performed. Membranes were removed by centrifugation before a final adjustment to 1× TEN salts with 2.5% NP-40–0.1% sodium dodecyl sulfate (SDS). Radiolabeled polypeptides were specifically immunoprecipitated and fractionated by SDS-polyacrylamide gel electrophoresis (PAGE) (10% acrylamide gel). Gels were visualized and analyzed using a Molecular Dynamics Typhoon Storm 860 PhosphorImager with ImageQuant software. The antibodies used for immunoprecipitation, rabbit anti-BiP and anti-VSG117, have been described previously (7, 8).

Endocytic activity in bloodstream trypanosomes was assessed by uptake of tomato lectin (TL). Cultured cells were washed and resuspended (5×10^6/ml) in serum-free HMI9 medium containing 1% bovine serum albumin (2). Cells were incubated for 1 h at 37°C in the presence of 20 μg/ml fluorescein isothiocyanate-conjugated TL (FITC-TL; Vector Laboratories, Burlingame, CA). Following uptake, cells were washed three times with ice-cold phosphate-buffered saline (PBS) containing 5% FBS and processed for immunofluorescence microscopy or flow cytometry.

Flow cytometry and immunofluorescence microscopy. For flow cytometry following uptake of FITC-TL, cells were fixed with PBS containing 2% formalydehyde for 15 to 30 min on ice, centrifuged, and resuspended in 1 ml PBS–5% FBS. Labeled cells were analyzed on a FACScan (Becton Dickinson, Mountain View, CA) using CellQuest software. For immunofluorescence microscopy, trypanosomes were smeared on glass slides, fixed, permeabilized, and stained as previously described (2). Specific staining was detected by appropriate Alexa 488- and Alexa 633-conjugated secondary antibodies (Molecular Probes, Seattle, WA), and 500 ng/ml 4′,6′-diamidino-2-phenylindole (DAPI) was included to visualize nuclear and kinetoplast DNA. Cells were analyzed on a motorized Zeiss Axioplan IIi with a rear-mounted excitation filter wheel, a triple-pass (DAPI/FITC/Texas Red) emission cube, and differential interference contrast (DIC) optics. Serial 0.2-μm image Z-stacks at a magnification of ×100 (PlanApo; numerical aperture, 1.4) were collected with a Zeiss AxioCam black-and-white charge-coupled device camera. Fluorescence images were deconvolved using a constrained iterative algorithm, pseudocolored, and merged using OpenLabs (version 4.1) software (Improvision, Inc., Lexington, MA).

Transferrin uptake and electron microscopy. Bloodstream cells (3×10^7) were washed with HEPES-buffered solution (HBS) and resuspended in 0.7 ml HMI9-bovine serum albumin. Tf-gold (0.3 ml bovine holotransferrin conjugated to 5-nm-diameter colloidal gold particles suspended in PBS to an optical density at 520 nm of 5.8; Aurion, Wageningen, The Netherlands) was added, and the cells were incubated at 37°C for 2 h, followed by a wash in HBS to remove unbound Tf-gold. Cells were then cultured (37°C, 14 h) in HMI9 with 20% FBS and with or without myriocin (200 nM) at 7.5×10^4/ml. Cells were washed again in HBS and then fixed in 2.5% glutaraldehyde–2.0% paraformaldehyde in 0.1 M sodium cacodylate buffer (pH 7.4) for ~20 h at 4°C. The cells were postfixed in 1% osmium tetroxide in the same buffer for 1 h at room temperature. Samples were then serially dehydrated in ethanol, transferred to propylene oxide, and flat-embedded in Spurr's epoxy resin (Electron Microscopy Sciences, Hatfield, PA). Sections (thickness, 60 to 90 nm) were cut on a Reichert-Jung Ultracut-E Ultramicrotome and contrasted with uranyl acetate in 50% ethanol. Ultrathin sections were mounted and observed with a Philips CM120 electron microscope. All images were captured with a MegaView III (Soft Imaging System, Lakewood, CO) side-mounted digital camera.

Intracellular trafficking in HeLa cells. To assay the trafficking of HA-GPI, cells were transfected with a plasmid encoding the ectodomain of influenza virus hemagglutinin (HA) fused to the C-terminal GPI attachment signal of the decay-accelerating factor protein (63). Transfection was done by electroporation as described previously (62). Transfected cells were allowed to recover for 36 to 48 h before being pulse-labeled with 200 μCi/ml [^{35}S]methionine-cysteine for 20 min and chased for 2 h in complete medium. Labeling was done in the presence or absence of myriocin or BFA after a 30-min preincubation. At the end of the chase, the cells were washed with ice-cold PBS and incubated on ice with 100 μg/ml tosylsulfonyl phenylalanyl chloromethyl ketone (TPCK)-treated trypsin for 30 min. Trypsinization was stopped by adding soybean trypsin inhibitor (300 μg/ml) to the cells and incubating for a further 10 min on ice. Cells were scraped, washed twice with ice-cold PBS containing 100 μg/ml trypsin inhibitor, resuspended in radioimmunoprecipitation assay buffer, and incubated with anti-HA antibodies followed by protein G beads. The bead-bound immunoprecipitate was washed, heated in sample buffer, and resolved by SDS-PAGE (10% gel). Gels were visualized using a PhosphorImager. To assay the trafficking of free GPI, HeLa cells were pulse-labeled with [2-^{3}H]mannose to generate radiolabeled GPI in the ER. Transport of GPI to the cell surface was monitored by periodate oxidation and TLC analysis exactly as described previously (9).

RESULTS

Sphingoid base synthesis is essential for the growth of trypanosomes. Studies of both yeast and mammalian cells have shown that ongoing sphingolipid synthesis is essential for cell proliferation (14). However, recent work with the kinetoplastid parasite *Leishmania* demonstrate that log-phase promastigote-

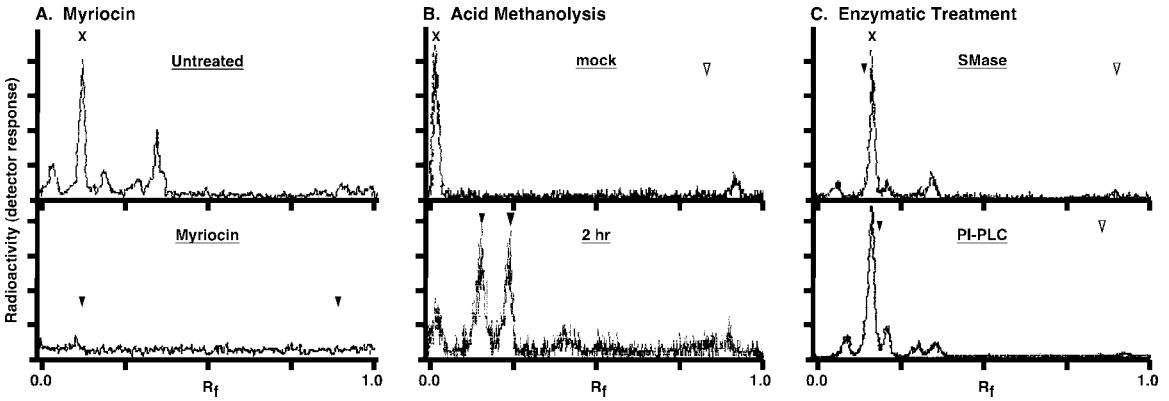

FIG. 2. Myriocin inhibition of de novo sphingolipid synthesis in trypanosomes. (A) Bloodstream-stage trypanosomes grown for 4 h in the presence (bottom) or absence (top) of 200 nM myriocin were pulse-radiolabeled with 50 μCi/ml of [^{3}H]serine for 4 h. Base-resistant lipids were extracted as described in Materials and Methods and analyzed by TLC. The mobilities of sphingomyelin (R_f, 0.12) and ceramide (R_f, 0.89) standards were determined by iodine staining (arrowheads, bottom panel only). (B) Saponified [^{3}H]serine-labeled lipids were subjected to mock treatment (top) or acid methanolysis (bottom) (2 h) as described in Materials and Methods and then analyzed by TLC. Ceramide was added as an internal marker/substrate prior to hydrolysis. The mobilities of unhydrolyzed ceramide (open arrowhead) (R_f, 0.83), the sphingosine product (shaded arrowhead) (R_f, 0.25), and the sphinganine product (solid arrowhead) (R_f, 0.15) are indicated. (C) Base-resistant [^{3}H]serine-labeled lipids from untreated bloodstream trypanosomes were either mock treated (not shown) or digested with either sphingomyelinase (SMase) (top) or bacterial PI-PLC (bottom) with internal sphingomyelin and PI controls, respectively. Samples were prepared and analyzed as for panel A. Solid arrowheads indicate relative mobilities of internal sphingomyelin (top) (R_f, 0.14) and PI (bottom) (R_f, 0.22) control substrates (from the mock treatments), and open arrowheads indicate the respective ceramide (top) (R_f, 0.9) and diacylglycerol (bottom) (R_f, 0.8) products. Note that the solvent systems used for panels A and C are different from that for panel B.

stage mutants lacking SPT activity fail to synthesize ceramides and sphingolipids yet show no marked growth defect compared to wild-type cells (17, 68), provided that they are supplemented with exogenous ethanolamine (67). In light of this key difference between *Leishmania* and other eukaryotes, we wanted to investigate the requirements for de novo sphingolipid synthesis for the growth of the closely related kinetoplastid *T. brucei*. Treatment of bloodstream-stage trypanosomes with myriocin, an inhibitor of sphingolipid synthesis (44), resulted in a dose-dependent inhibition of growth with a 50% inhibitory concentration of ~100 to 150 nM (Fig. 1B). Procyclic-stage trypanosomes showed a similar myriocin-induced growth inhibition, albeit with a higher 50% inhibitory concentration (~800 nM) (data not shown).

We wanted to determine if myriocin-induced growth inhibition was due to a block at a specific cell cycle checkpoint. Most trypanosomes in an asynchronously growing population are in interphase and contain a single kinetoplast (mitochondrial genome) and nucleus (1k/1n). During cell division, the kinetoplast divides, first generating intermediates with two kinetoplasts and a single nucleus (2k/1n); this is followed by nuclear division to produce cells with two kinetoplasts and two nuclei (2k/2n). Finally, cytokinesis results in two interphase daughter cells (26). Microscopic examination of myriocin-treated bloodstream cells stained for DNA with DAPI showed a decrease in the proportion of interphase cells (1k/1n) with a concomitant increase in the products of aberrant cell division (1k/0n, 1k/2n, and >2k/>2n) compared to untreated control cells (Fig. 1C). These results indicate that myriocin treatment of bloodstream trypanosomes leads to arrest of cell growth at all stages of the cell cycle.

The first step in sphingolipid biosynthesis, catalyzed by SPT, produces the sphingoid base 3-KDS, which is converted to sphinganine (dihydrosphingosine) and then N acylated and desaturated to generate ceramide, the immediate precursor for all higher-order sphingolipids (Fig. 1A). Addition of 3-KDS completely rescued the myriocin-induced growth inhibition (Fig. 1D), indicating that the defect is not due to general toxicity but rather is specifically due to inhibition of ongoing sphingoid base synthesis by SPT. In contrast, addition of ceramide failed to rescue cell growth, likely due to inefficient uptake and/or delivery of exogenous ceramide to the Golgi apparatus, consistent with previous observations of mammalian cells and *Leishmania* (30, 68). Growth and differentiation defects observed in *Leishmania* promastigote mutants lacking either SPT or sphingosine-1-phosphate lyase (SPL) activity can be rescued by exogenous ethanolamine (67). This issue is discussed in detail below, but briefly, the basis for the phenomenon is believed to be acquisition of essential ethanolamine via SPL activity (Fig. 1A). Loss of sphingoid base synthesis leads to ethanolamine auxotrophy by depletion of sphingosine-1-phosphate. However, African trypanosomes appear to differ from *Leishmania* in this respect; addition of ethanolamine was unable to rescue growth for either procyclic (data not shown) or bloodstream (Fig. 1D) cells.

De novo sphingolipid synthesis is inhibited by myriocin. In order to confirm that myriocin-induced growth inhibition is due to a block in de novo sphingoid base synthesis, we metabolically radiolabeled bloodstream-form trypanosomes with [^{3}H]serine and extracted base-resistant cellular lipids for analysis by thin layer chromatography (Fig. 2A). Myriocin-treated cells showed a decrease in total protein synthesis (trichloroacetic acid-insoluble incorporation of [^{3}H]serine) of ~25% compared to untreated control cells, indicating that the compound had minimal effect on general metabolic function (data not shown). In control, untreated cells (Fig. 2A, top panel), a single major radiolabeled lipid (designated X) was detected, as well as several variable minor peaks (Fig. 2, compare panels A

and C), and myriocin treatment completely blocked incorporation into all of these species (bottom panel). The combined base resistance and myriocin sensitivity of all the labeled peaks indicate that they are sphingolipids. This was verified by acid methanolysis, which released radiolabeled products that comigrated with sphingosine and sphinganine in TLC analysis (Fig. 2B). Sphingolipid X routinely migrated slightly ahead of the sphingomyelin marker in our standard solvent system (CMW, 65:25:4; R_f, 1.2 to 1.4 for sphingomyelin versus 1.5 to 1.7 for sphingolipid X), suggesting that it is a distinct species. Consistent with this, neither sphingolipid X nor the other radiolabeled sphingolipids were sensitive to hydrolysis by sphingomyelinase (Fig. 2C, top). In addition, bacterial PI-PLC, which is known to hydrolyze inositol phosphorylceramide from *T. cruzi* (1, 11), had no effect on sphingolipid X (Fig. 2C, bottom), indicating that it is not IPC. These results indicate that myriocin effectively blocks de novo synthesis of sphingoid bases, and they further suggest that bloodstream-stage African trypanosomes may synthesize a novel higher-order sphingolipid.

De novo sphingolipid synthesis is not required for forward transport in trypanosomes. Ongoing sphingolipid synthesis is required for efficient ER exit of GPI-anchored proteins in yeast (33, 59). We wanted to examine whether there is a similar requirement for sphingolipids in the forward transport of GPI-anchored proteins in bloodstream-form trypanosomes. First, we characterized the forward transport of a non-GPI-anchored protein in order to determine if myriocin treatment had any globally deleterious effects on transport. We have previously characterized the kinetics of protein secretion in bloodstream trypanosomes by using the soluble recombinant protein BiPN, based on the ATPase domain of endogenous BiP (60). In agreement with our previous results, we find that BiPN is detected at the beginning of the chase period (T_0) as a ~45-kDa cell-associated polypeptide in control cells (Fig. 3A, lane 1). In addition, full-length endogenous BiP with associated nascent VSG is also detected (5). During the chase, BiPN, but not endogenous BiP, is efficiently (~50% after 2 h) exported to the medium (Fig. 3A, lanes 7 and 11). In addition, BiP-associated VSG disappeared at later time points as normally expected for a nascent secretory polypeptide (Fig. 3A, lanes 5 and 9). Myriocin treatment had no qualitative or quantitative effects on synthesis of BiP, VSG, or BiPN (Fig. 3A, lane 2) or on BiPN secretion (lanes 8 and 12). These results indicate that despite the dramatic inhibition of cell proliferation, shutdown of sphingoid base synthesis does not disrupt the synthesis or transport of a non-GPI-anchored secretory reporter protein.

Next, we used pulse-chase analysis to determine the effects of myriocin treatment on the kinetics of ER-to-surface transport of GPI-anchored VSG (Fig. 3B). The arrival of VSG at the surface was measured by an indirect assay that relies on the differential accessibility of mature surface VSG versus newly synthesized internal VSG to cleavage by endogenous GPI-PLC. When cells are lysed by hypotonic lysis, endogenous GPI-PLC cleaves accessible GPI-anchored VSG to a soluble form, which is released from cells (15). Kinetically, susceptibility to GPI hydrolysis during hypotonic lysis coincides with the arrival of VSG at the cell surface ($t_{1/2}$, ~15 min) (4). In close agreement with the known rate, newly synthesized VSG was highly resistant to release by hypotonic lysis (Fig. 3B, lane 2) but became completely sensitive over a 30-min chase (lanes 3 to 5). Myriocin treatment had no significant effect on this process (Fig. 3B, lanes 8 to 11), indicating that efficient ER exit and subsequent transport through the secretory pathway of GPI-anchored VSG are not dependent on ongoing sphingolipid synthesis.

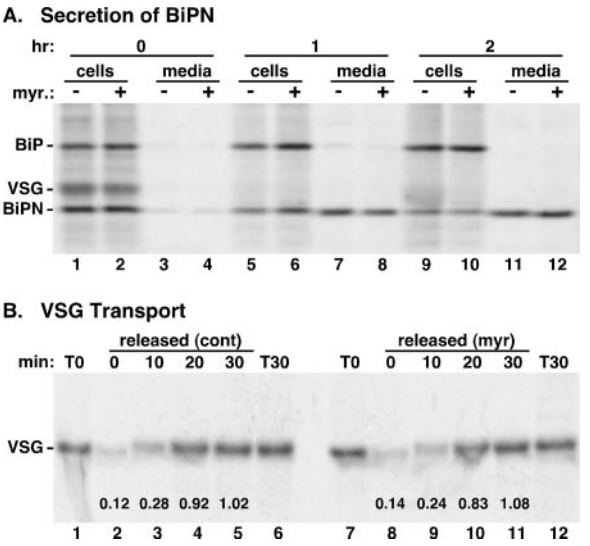

FIG. 3. Myriocin does not block secretory transport in trypanosomes. (A) Bloodstream-form trypanosomes constitutively expressing the soluble secretory reporter BiPN were cultured for 14 h in the absence (−) or presence (+) of 200 nM myriocin (myr.). Cells were pulse-radiolabeled (15 min) with [^{35}S]Met-Cys and then chased for the indicated times in the continued presence or absence of the inhibitor. The BiPN reporter was immunoprecipitated from cell and medium fractions and analyzed by SDS-PAGE and phosphorimaging. The mobilities of endogenous BiP and VSG, and of the BiPN reporter, are indicated on the left. All lanes contain 5×10^6 cell equivalents. Note that the time points used in this assay fall in the linear range for BiPN transport in bloodstream cells (60). (B) Bloodstream cells were cultured for 14 h in the presence or absence of 200 nM myriocin. Cells were then pulse-radiolabeled (3 min) with [^{35}S]Met-Cys and chased in the continued presence (myr) or absence (control [cont]) of the inhibitor. At the indicated times, samples were washed and subjected to hypotonic lysis as described in Materials and Methods, and VSG polypeptides were immunoprecipitated from the released fractions. VSG was also immunoprecipitated from total-cell fractions at the beginning and end of the chase period (T_0 and T_{30}), and all samples were analyzed as for panel A. The recovery of released VSG as a fraction of total VSG (average of T_0 and T_{30}) is given for each lane. All lanes contain 2×10^6 cell equivalents.

Sphingolipid synthesis is required for endocytosis in trypanosomes. Temperature-sensitive SPT mutants in yeast show a defect in endocytosis (65), but the connection between ongoing synthesis of sphingoid bases and endocytosis remains to be fully defined. Consequently, we investigated whether myriocin treatment of bloodstream trypanosomes would affect endocytosis. Since myriocin treatment led to an observable decrease in cell motility and a fattening of the cell shape, we first visualized the localization of two key organelles in the secretory/endocytic pathway, the ER and the lysosome, by immunofluorescence microscopy (Fig. 4A to H). In both control and myriocin-treated cells, staining with anti-BiP (Fig. 4B and F) revealed a fine reticulated network characteristic of the ER, and staining with an antibody to the lysosomal membrane protein p67 (Fig. 4C and G) revealed a vesicular compartment

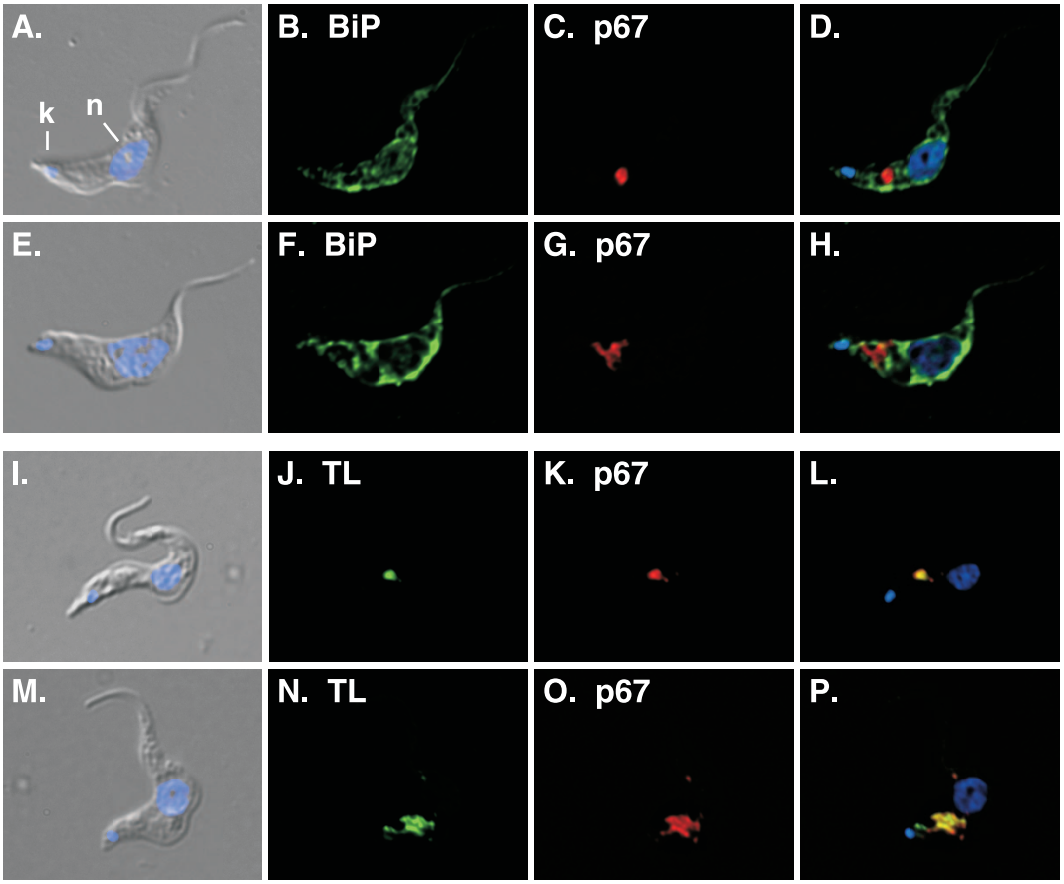

FIG. 4. Myriocin disrupts lysosomal morphology in trypanosomes. Bloodstream-form trypanosomes were cultured for 14 h in the presence or absence of myriocin (200 nM). Fixed/permeabilized control (A to D) and myriocin-treated (14 h) (E to H) cells were stained with anti-BiP as an ER marker (green) (B and F) or anti-p67 as a lysosomal marker (red) (C and G) and were visualized by epifluorescence microscopy. Alternatively, control (I to L) and myriocin-treated (M to P) cells were allowed to endocytose FITC-TL (J and N) for 1 h and were then processed for staining with anti-p67 (K and O). (A, E, I, and M) Merged DIC and DAPI images; (D, H, L, and P) merged three-channel fluorescent images. DAPI staining (blue) reveals nucleus (n) and kinetoplast (k) localization (indicated in panel A only).

located properly between the nucleus and the kinetoplast. However, compared to control cells, the majority of myriocin-treated cells showed a distorted and enlarged $p67^+$ compartment (Fig. 4G and O). To more carefully investigate the effects of myriocin on trypanosomal ultrastructure, we performed transmission electron microscopy using Tf-gold as a lysosomal marker. Cells were preloaded with Tf-gold to label the terminal lysosome and were then treated with myriocin. In untreated control cells, lysosomes typically had diameters of ~300 nm (Fig. 5A, B, E, and F). In contrast, myriocin-treated cells typically exhibited lysosomes with diameters of >600 nm (Fig. 5C, D, G, and H). No other obvious ultrastructural abnormalities were observed in myriocin-treated cells. These results confirm that lysosomal morphology is altered, and they imply that ongoing sphingolipid synthesis may play a role in membrane trafficking events involved in the formation and/or maintenance of the lysosomal compartment.

We used the uptake of FITC-TL to assess receptor-mediated endocytosis (Fig. 4I to P). Tomato lectin binds poly-*N*-acetyllactosamine-containing N-glycans on membrane glycoproteins in the flagellar pocket of bloodstream trypanosomes (46). Many of these glycoproteins are internalized into the endocytic pathway, and TL eventually accumulates in the terminal lysosomal compartment (2). Microscopic analysis of TL uptake failed to detect any obvious defects in lysosomal delivery; the majority of internalized TL colocalized completely with the resident lysosomal protein p67 in both untreated and myriocin-treated cells (Fig. 4L and P). The distribution of internalized TL is more diffuse in myriocin-treated cells, presumably due to the enlarged lysosomal compartment. Next, we employed a quantitative assay using flow cytometry to measure the uptake of FITC-TL. Bloodstream cells pretreated for 4 h with myriocin were similar to untreated cells in their ability to take up TL (Fig. 6A). However, after a 14-h myriocin pretreatment, cells showed a significant decrease in the uptake of TL compared to untreated cells (Fig. 6B). Collectively these results suggest that sphingolipids play an important role in endocytosis.

Sphingolipid synthesis and intracellular transport in mammalian cells. In contrast to the situation for yeast (50, 59, 65), ER exit and intracellular transport of GPI-anchored proteins in trypanosomes apparently does not require ongoing de novo synthesis of sphingolipids. To further investigate this issue in a broader biological context, we assessed the effects of myriocin

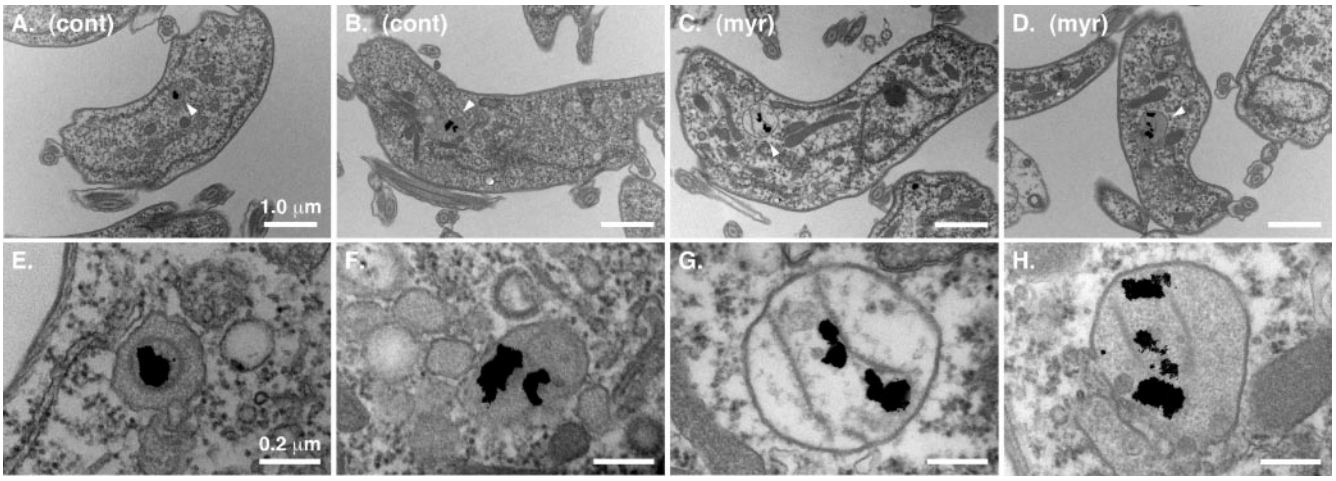

FIG. 5. Ultrastructure of myriocin-treated trypanosomes. Cultured bloodstream cells were first pulse-loaded (2 h, 37°C) with colloidal gold (5 nm) coupled to bovine holotransferrin to label the terminal lysosome. Cells were then cultured in the absence (A and B) or presence (C and D) of myriocin (200 nM) for 14 h and processed as described for electron microscopy. (A to D) Representative cell sections. Bar, 1.0 μm. White arrowheads indicate lysosomes containing colloidal gold particles. cont, control; myr, myriocin. (E to H) Corresponding images in the lysosomal region taken at a higher magnification. Bar, 0.2 μm.

on sphingolipid synthesis and GPI transport in mammalian HeLa cells. First, we determined that myriocin indeed blocks the incorporation of [^{3}H]serine into sphingomyelin and glucosylceramide (data not shown), confirming its inhibitory activity in HeLa cells. Next, we measured the transport of a GPI-anchored influenza virus hemagglutinin reporter (HA-GPI) by pulse-chase analysis in transiently transfected HeLa cells (Fig. 7). In this assay, the arrival of the reporter at the cell surface is measured by susceptibility to discrete cleavage by exogenously added trypsin to yield a diagnostic HA2 fragment.

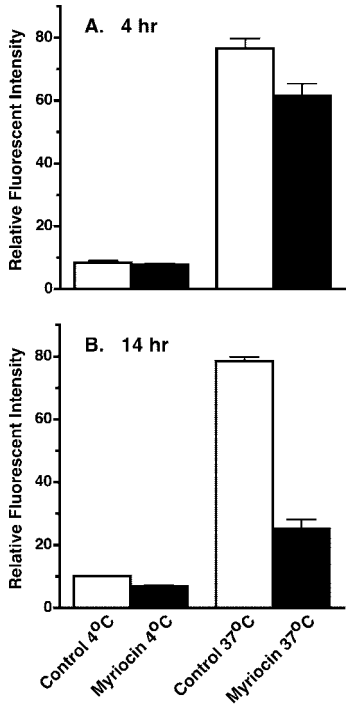

FIG. 6. Myriocin affects endocytic transport in trypanosomes. Bloodstream cells were cultured for 4 h (A) or 14 h (B) in the presence or absence of 200 nM myriocin. Cells were then incubated at 4°C or 37°C for 1 h in a medium containing 20 μg/ml FITC-tomato lectin, washed, and analyzed by flow cytometry. Uptake is presented as relative fluorescent intensity, in arbitrary units. Values are means ± standard deviations from three independent experiments.

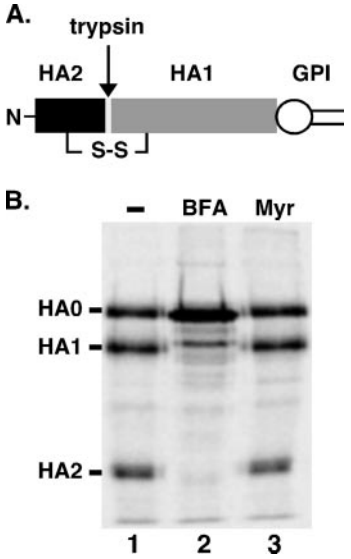

FIG. 7. Transport of HA-GPI to the plasma membranes of HeLa cells is unaffected by myriocin treatment. (A) Schematic representation of HA-GPI. The protein is synthesized as a GPI-anchored polypeptide (HA0, corresponding to the ectodomain of influenza virus hemagglutinin protein) containing a disulfide bond as shown. Upon trypsin treatment, HA0 yields two disulfide-linked fragments, HA2 and HA1. (B) HeLa cells expressing HA-GPI were preincubated for 30 min with myriocin (125 μM) or BFA (5 μg/ml) as indicated and were then pulse-labeled with 200 μCi/ml [^{35}S]methionine-cysteine for 20 min. The cells were chased for 2 h in the presence of drugs before being trypsinized to convert cell surface HA-GPI molecules into HA2 and HA1. The extent of conversion of radiolabeled protein to HA2 and HA1 was determined after immunoprecipitation and SDS-PAGE. A scan of a typical fluorography is presented. No HA2 is seen in the BFA-treated cells, whereas radiolabeled HA2 is readily observed in both control (−) and myriocin-treated cells.

At the end of the chase period, the reporter is as sensitive to trypsin in the presence of myriocin (Fig. 7B, lane 3) as it is in control cells (lane 1), indicating that transport is unimpeded when de novo sphingolipid synthesis is blocked. In control cells treated with brefeldin A, an inhibitor of vesicular secretory trafficking (21), HA-GPI cleavage is completely blocked (Fig. 7B, lane 2), confirming the validity of the assay. Finally, we measured the effect of myriocin treatment on the trafficking of [^{3}H]mannose-labeled free GPI, a process that we have previously demonstrated to be dependent on vesicular trafficking (9). In this assay, the arrival of free GPI of a known structure (H8) (Fig. 8A) at the cell surface is determined by susceptibility to oxidation by exogenously added metaperiodate, which is impermeant to intact biological membranes. Following an extended chase period, periodate treatment converts a substantial portion of [^{3}H]mannose-labeled GPI H8 to the oxidized H8* form (Fig. 8B). More-precise kinetic analysis indicates that myriocin treatment has no effect on the susceptibility of H8 to oxidation throughout the linear range for transport to the cell surface, while brefeldin A treatment completely abrogates periodate sensitivity (Fig. 8C). Collectively these data indicate that in mammalian cells, as in bloodstream trypanosomes, de novo synthesis of sphingolipids is not necessary for the transport of GPI structures at any stage of the secretory pathway.

DISCUSSION

The most current models of GPI-dependent protein sorting are based on the lateral association of GPI-anchored proteins (and free GPI) with ceramide or sphingolipid/sterol-rich microdomains (lipid rafts), which are proposed to act as selective platforms for vesicle budding at different sites along the secretory and endocytic pathways (56, 57). Consistent with these models, ceramide synthesis is required for both efficient membrane association and ER exit of GPI-anchored proteins in yeast (3, 59). We have investigated the universality of these concepts for the trafficking of GPI-anchored proteins and free GPI in two systems representing the broad sweep of eukaryotic evolution, African trypanosomes and nonpolarized human HeLa cells. In contrast to the prevailing view on the role of sphingolipids in secretory trafficking, we find for both systems that ER exit and transport to the cell surface of GPI-anchored proteins occur in the absence of ongoing sphingolipid synthesis. In addition, we have found a similar lack of effect on secretory trafficking in procyclic insect-stage trypanosomes (data not shown). We cannot rule out the possibility that ongoing transport is supported by the pool of ceramide and sphingolipid synthesized prior to treatment with myriocin, but nevertheless, de novo synthesis of sphingoid bases is clearly not required.

It should be noted that similar studies using both pharmacological and genetic strategies to block sphingolipid synthesis have been performed on *Leishmania*. Myriocin had no effect on overall ER-to-plasma membrane transport or on the incorporation into surface DRMs of free GPI or the major surface GPI-anchored protein GP63 (52). Similarly, genetic ablation of a subunit of SPT, which prevents sphingoid base synthesis, did not perturb the overall transport of GP63 or its association with plasma membrane DRMs (17, 68). Denny and coworkers performed a more detailed kinetic assay that revealed a decrease in the rate of association of newly synthesized GP63 with DRMs, suggesting a role for lipid rafts in ER exit (17); however, this finding could not be reproduced by others (66).

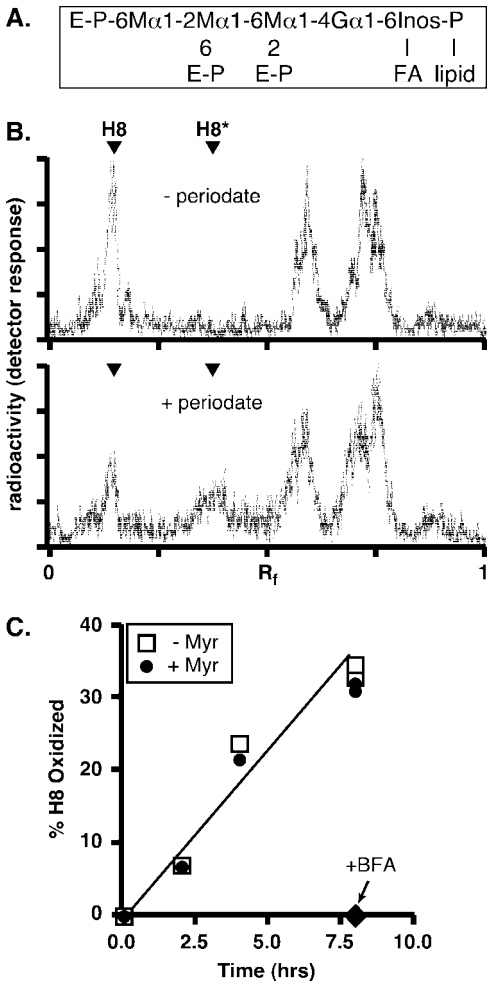

FIG. 8. Transport of free GPIs to the cell surface in HeLa cells is unaffected by myriocin. (A) Structure of the mammalian GPI H8, showing glycosidic linkages and sites of ethanolamine-phosphate (E-P) attachment. M, mannose; G, glucosamine; Inos, inositol; FA, fatty acid. (B) HeLa cells were first preincubated in a low-glucose medium with 6 μg/ml tunicamycin for 30 min at 37°C, then metabolically radiolabeled with [2-^{3}H]mannose for 2.5 h at 37°C, and finally chased for 18 h in complete medium. At the end of the chase period, the cells were washed, incubated for 30 min on ice in PBS (without [−] or with [+] 10 mM sodium metaperiodate), and washed again in PBS supplemented with 150 mM glycerol. The cells were collected, and lipids were extracted and analyzed by TLC (chloroform-methanol-water, 10:10:3 [vol/vol/vol]). [^{3}H]mannose-labeled H8 migrates with an R_f of ~0.25 (the identity of H8 was confirmed by establishing its sensitivity to hydrolysis by GPI-specific phospholipase D [not shown]). Periodate treatment (lower panel) converts ~50% of H8 to oxidized H8 (H8*). Several faster-migrating radiolabeled peaks were unaffected by periodiate, suggesting that these unidentified species are intracellular. (C) HeLa cells were first preincubated with myriocin (25 μg/ml) for 20 min, then pulse-labeled with [2-^{3}H]mannose, and finally chased for 8 h in complete medium containing 62.5 μM myriocin (+ Myr). Control (untreated) (− Myr) and BFA-treated samples (cells were preincubated with BFA [2.5 μg/ml] and chased in the presence of the drug) were analyzed in parallel. Cells were taken at different time points and subjected to periodate oxidation to determine the fraction of radiolabeled H8 that was transported from the ER and located at the cell surface.

Thus, the results for *Leishmania* are contradictory. So is the evidence for association of GPI-anchored proteins with DRMs in African trypanosomes. Nolan et al. reported that VSG does not significantly associate with DRMs, while Denny et al. found such association by using a lower detergent concentration (16, 47). Consequently, the existence of DRMs in trypanosomes must be more systemically investigated before an assessment of the role of lipid rafts in VSG and GPI trafficking in trypanosomes can be made. Whatever the status of DRMs in *T. brucei*, or the situation in *Leishmania*, our results for African trypanosomes and HeLa cells clearly establish that ongoing sphingolipid synthesis is not a universal requirement for forward transport of GPI-anchored proteins in eukaryotic cells.

On the other hand, we do find a general defect in endocytosis for African trypanosomes when sphingolipid synthesis is blocked. Typically, newly synthesized sphingolipids traffic as ceramide from the ER to the Golgi apparatus, where higher-order modifications occur, and then on to the plasma membrane (64). Consequently, it seems unlikely that inhibition of sphingoid base synthesis would lead to rapid depletion of sphingolipids at the plasma membrane. Consistent with this notion, pulse-chase analysis indicates only minor turnover of [^{3}H]serine-labeled sphingolipid X over a 14-h period in both control and myriocin-treated cells (~10% [data not shown]). Thus, our results argue that a prolonged myriocin treatment is required before defects in endocytosis are detected. This is in contrast to the situation for yeast, where a sphingoid base-mediated signaling pathway rapidly regulates endocytosis through protein phosphorylation (25, 65). Although we cannot rule out secondary effects due to prolonged inhibition, the time frame of our results for trypanosomes is more consistent with a general role for sphingolipids in cellular membranes.

One surprising implication of our studies is that bloodstream-stage African trypanosomes may synthesize unusual sphingolipids. After the production of ceramide in the ER, eukaryotes go on to synthesize a diverse array of higher-order sphingolipids. Many of the lower eukaryotes, including fungi (38) and the kinetoplastids *Leishmania* (35) and *Trypanosoma cruzi* (54), synthesize IPC, and it has been generally assumed that African trypanosomes likewise synthesize IPC (18, 19, 32). In fact, earlier compositional analyses of African trypanosomes found no evidence for IPC; rather, sphingomyelin was detected at fairly high levels in bloodstream-stage parasites (49). Although the presence of IPC in procyclic trypanosomes has recently been confirmed (27), our results suggest that neither sphingomyelin nor IPC is made by bloodstream-form *T. brucei* in our biosynthetic assays, and they raise the possibility of developmental regulation of sphingolipid synthesis. The nature of the major sphingolipid detected in our biosynthetic assays remains uncertain. The close but imprecise migration of sphingolipid X with authentic sphingomyelin in TLC analyses could account for the previous identification of sphingomyelin in compositional analyses. Alternatively, sphingolipid X may be related to one of the recently identified neutral glycosphingolipids in *T. brucei* (61). Although further structural work is needed to identify this lipid, our analyses suggest that African trypanosomes synthesize novel sphingolipids relative to their kinetoplastid brethren.

African trypanosomes also differ from *Leishmania* in two additional ways: growth dependence on sphingoid base synthesis and rescue of sphingoid base deficiency with exogenous ethanolamine. *SPT*-null *Leishmania* parasites replicate well as log-phase promastigotes but differentiate poorly to infectious stationary-phase metacyclic promastigotes (17, 68). Thus, de novo synthesis of sphingoid bases is apparently not necessary for replicative growth in vitro but is necessary for differentiation. However, Zhang and coworkers have recently found that *SPT* is absolutely essential for growth under conditions that are strictly limiting for exogenous phospholipids (67). Interestingly, the defect in differentiation can be complemented by exogenous ethanolamine, and furthermore, the same phenotype, including rescue by ethanolamine, can be duplicated in an *SPL*-null mutant. The likely explanation for these related phenotypes is that cleavage of sphingosine-1-phosphate, a downstream product of SPT activity, generates essential ethanolamine phosphate (EtN-P) for anabolic purposes such as phosphatidylethanolamine synthesis via the Kennedy pathway (reaction 1, EtN-P + CTP $\rightarrow$ CDP:EtN + PP_i; reaction 2, CDP:EtN + DAG $\rightarrow$ PE + CMP [36, 37]). A major implication of this finding is that *Leishmania* is not dependent on de novo synthesis of higher-order sphingolipids, e.g., IPC, for growth, viability and virulence.

Unlike *Leishmania*, however, African trypanosomes are critically dependent on de novo synthesis of sphingolipids. The trivial explanation for our major finding, that myriocin toxicity is due to nonspecific side effects, is ruled out because the immediate product of SPT activity, 3-KDS, completely rescues cell viability. Although *T. brucei* has an orthologue (Tb927.6.3630) of the *Leishmania SPL* gene, our data suggest that the deleterious effect of blocking sphingoid base synthesis is not due to ethanolamine deficiency either, since exogenous ethanolamine is unable to complement growth. Nor can this be due to a deficiency in uptake, since exogenous ethanolamine is readily transported and incorporated into GPI and phospholipids (42, 53). The failure of exogenous ethanolamine to rescue myriocin toxicity does not rule out the possibility that trypanosomes also acquire ethanolamine via the SPL pathway, but clearly sphingoid base synthesis is required for some other purpose. The obvious candidates are ceramide and higher-order sphingolipids, presumably as important structural components of cell membranes. Precisely what these higher-order sphingolipids are in African trypanosomes, and how they relate to the lipids detected in our biosynthetic assays, will require careful structural characterization of steady-state lipids in both life cycle stages of these unusual parasites.

ACKNOWLEDGMENTS

We are indebted to Steve Beverley and Kai Zhang for thoughtful discussions and sharing of unpublished data. We thank Debbie Brown (SUNY, Stony Brook, NY) for suggesting the HA-GPI trafficking assay, Saulius Vainauskas for the HA-GPI construct (originally obtained from Judy White, University of Virginia), Niki Baumann for input on the initial experiments with GPI trafficking in HeLa cells, Henna Ohvo-Rekilä for assistance with sphingolipid analysis, Dawn Ransom for the initial myriocin experiment on trypanosomes, and Kevin Schwartz for technical assistance with parasites. We also thank the staff at the UW Medical School Electron Microscopy Facility, particularly Ben August, for technical assistance and helpful suggestions in performing electron microscopy.

This work was supported by National Institutes of Health grants AI35739 (to J.D.B.) and GM55427 (to A.K.M.) and the Cornell/

Rockefeller/Sloan-Kettering Tri-Institutional Training Program in Chemical Biology (to S.S.).

REFERENCES

1. **Agusti, R., A. S. Couto, O. Campetella, A. C. C. Frasch, and R. M. de Lederkremer.** 1998. Structure of the glycosylphosphatidylinositol-anchor of the *trans*-sialidase from *Trypanosoma cruzi* metacyclic trypomastigote forms. Mol. Biochem. Parasitol. **97:**123–131.
2. **Alexander, D. L., K. J. Schwartz, A. E. Balber, and J. D. Bangs.** 2002. Developmentally regulated trafficking of the lysosomal membrane protein p67 in *Trypanosoma brucei*. J. Cell Sci. **115:**3253–3263.
3. **Bagnat, M., S. Keränen, A. Shevchenko, A. Shevchenko, and K. Simons.** 2000. Lipid rafts function in biosynthetic delivery of proteins to the cell surface in yeast. Proc. Natl. Acad. Sci. USA **97:**3254–3259.
4. **Bangs, J. D., N. Andrews, G. W. Hart, and P. T. Englund.** 1986. Posttranslational modification and intracellular transport of a trypanosome variant surface glycoprotein. J. Cell Biol. **103:**255–263.
5. **Bangs, J. D., E. M. Brouch, D. M. Ransom, and J. L. Roggy.** 1996. A soluble secretory reporter system in *Trypanosoma brucei*: studies on endoplasmic reticulum targeting. J. Biol. Chem. **271:**18387–18393.
6. **Bangs, J. D., D. Herald, J. L. Krakow, G. W. Hart, and P. T. Englund.** 1985. Rapid processing of the carboxyl terminus of a trypanosome variant surface glycoprotein. Proc. Natl. Acad. Sci. USA **82:**3207–3211.
7. **Bangs, J. D., D. M. Ransom, M. A. McDowell, and E. M. Brouch.** 1997. Expression of bloodstream variant surface glycoproteins in procyclic stage *Trypanosoma brucei*: role of GPI anchors in secretion. EMBO J. **16:**4285–4294.
8. **Bangs, J. D., L. Uyetake, M. J. Brickman, A. E. Balber, and J. C. Boothroyd.** 1993. Molecular cloning and cellular localization of a BiP homologue in *Trypanosoma brucei*: divergent ER retention signals in a lower eukaryote. J. Cell Sci. **105:**1101–1113.
9. **Baumann, N. A., J. Vidugiriene, C. A. Machamer, and A. K. Menon.** 2000. Cell surface display and intracellular trafficking of free glycosylphosphatidylinositols in mammalian cells. J. Biol. Chem. **275:**7378–7389.
10. **Bertello, L., M. F. Goncalvez, W. Colli, and R. M. de Lederkremer.** 1995. Structural analysis of inositol phospholipids from *Trypanosoma cruzi* epimastigote forms. Biochem. J. **310:**255–261.
11. **Bertello, L. E., M. J. M. Alves, W. Colli, and R. M. de Lederkremer.** 2000. Evidence for phospholipases from *Trypanosoma cruzi* active on phosphatidylinositol and inositolphosphoceramide. Biochem. J. **345:**77–84.
12. **Brown, D. A., B. Crise, and J. K. Rose.** 1989. Mechanism of membrane anchoring affects polarized expression of two proteins in MDCK cells. Science **245:**1499–1501.
13. **Brown, D. A., and E. London.** 1998. Functions of lipid rafts in biological membranes. Annu. Rev. Cell Dev. Biol. **14:**111–136.
14. **Cerbon, J., A. Falcon, C. Hernandez-Luna, and D. Segura-Cobos.** 2005. Inositol phosphoceramide synthase is a regulator of intracellular levels of diacylglycerol and ceramide during the G_1 to S transition in *Saccharomyces cerevisiae*. Biochem. J. **388:**169–176.
15. **Cross, G. A. M.** 1984. Release and purification of *Trypanosoma brucei* variant surface glycopotein. J. Cell. Biochem. **24:**79–90.
16. **Denny, P. W., M. C. Field, and D. F. Smith.** 2001. GPI-anchored proteins and glycoconjugates segregate into lipid rafts in Kinetoplastida. FEBS Lett. **491:**148–153.
17. **Denny, P. W., D. Goulding, M. A. Ferguson, and D. F. Smith.** 2004. Sphingolipid-free *Leishmania* are defective in membrane trafficking, differentiation and infectivity. Mol. Microbiol. **52:**313–327.
18. **Denny, P. W., H. Shams-Eldin, H. P. Price, D. F. Smith, and R. T. Schwarz.** 2006. The protozoan inositol phosphorylceramide synthase: a novel drug target which defines a new class of sphingolipid synthase. J. Biol. Chem. **281:**28200–28209.
19. **Denny, P. W., and D. F. Smith.** 2004. Rafts and sphingolipid biosynthesis in the kinetoplastid parasitic protozoa. Mol. Microbiol. **53:**725–733.
20. **Doering, T. L., and R. Schekman.** 1996. GPI anchor attachment is required for Gas1p transport from the endoplasmic reticulum in COP II vesicles. EMBO J. **15:**182–191.
21. **Donaldson, J. G., D. Finazzi, and R. D. Klausner.** 1992. Brefeldin A inhibits Golgi membrane-catalyzed exchange of guanine nucleotide onto ARF protein. Nature **360:**350–352.
22. **Duszenko, M., I. Ivanov, M. A. J. Ferguson, H. Plesken, and G. A. M. Cross.** 1988. Intracellular transport of a variant surface glycoprotein in *Trypanosoma brucei*. J. Cell Biol. **106:**77–86.
23. **Ferguson, M. A. J.** 1999. The structure, biosynthesis and functions of glycosylphosphatidylinositol anchors, and the contributions of trypanosome research. J. Cell Sci. **112:**2799–2809.
24. **Ferguson, M. A. J., M. Duszenko, G. S. Lamont, P. Overath, and G. A. M. Cross.** 1986. Biosynthesis of *Trypanosoma brucei* variant surface glycoprotein. *N*-glycosylation and addition of a phosphatidylinositol membrane anchor. J. Biol. Chem. **261:**356–362.
25. **Friant, S., R. Lombardi, T. Schmelzle, M. N. Hall, and H. Riezman.** 2001. Sphingoid base signaling via Pkh kinases is required for endocytosis in yeast. EMBO J. **20:**6783–6792.
26. **Gull, K., C. Birkett, R. Gerke-Bonet, A. Parma, D. Robinson, T. Sherwin, and R. Woodward.** 1990. The cell cycle and cytoskeletal morphogenesis in *Trypanosoma brucei*. Biochem. Soc. Trans. **18:**720–722.
27. **Güther, M. L. S., S. Lee, L. Tetley, A. Acosta-Serrano, and M. A. J. Ferguson.** 2006. GPI anchored proteins and free GPI glycolipids of procyclic form *Trypanosoma brucei* are non-essential for growth, are required for colonization of the tsetse fly and are not the only components of the surface coat. Mol. Biol. Cell **17:**5265–5274.
28. **Haldar, K.** 1996. Sphingolipid synthesis and membrane formation by *Plasmodium*. Trends Cell Biol. **6:**398–405.
29. **Hanada, K.** 2003. Serine palmitoyltransferase, a key enzyme in sphingolipid metabolism. Biochim. Biophys. Acta **1632:**16–30.
30. **Hanada, K., M. Nishijima, M. Kiso, A. Hasegawa, S. Fujita, T. Ogawa, and Y. Akamatsu.** 1992. Sphingolipids are essential for the growth of Chinese hamster ovary cells. Restoration of the growth of a mutant defective in sphingoid base biosynthesis by exogenous sphingolipids. J. Biol. Chem. **267:**23527–23533.
31. **Hancock, J. F.** 2006. Lipid rafts: contentious only from simplistic standpoints. Nat. Rev. Mol. Cell Biol. **7:**456–462.
32. **Heung, L. J., C. Luberto, and M. Del Poeta.** 2006. Role of sphingolipids in microbial pathogenesis. Infect. Immun. **74:**28–39.
33. **Horvath, A., C. Sutterlin, U. Manning-Krieg, N. Roa Movva, and H. Riezman.** 1994. Ceramide synthesis enhances transport of GPI-anchored proteins to the Golgi apparatus in yeast. EMBO J. **13:**3687–3695.
34. **Ikonen, E.** 2001. Roles of lipid rafts in membrane transport. Curr. Opin. Cell Biol. **13:**470–477.
35. **Kaneshiro, E. S., K. Jayasimhulu, and R. L. Lester.** 1986. Characterization of inositol lipids from *Leishmania donovani* promastigotes: identification of an inositol sphingophospholipid. J. Lipid Res. **27:**1294–1303.
36. **Kennedy, E. P.** 1956. The synthesis of cytidine diphosphate choline, cytidine diphosphate ethanolamine, and related compounds. J. Biol. Chem. **222:**185–192.
37. **Kennedy, E. P., and S. B. Weiss.** 1956. The function of cytidine coenzymes in the biosynthesis of phospholipids. J. Biol. Chem. **222:**193–214.
38. **Lester, R. L., and R. C. Dickson.** 1993. Sphingolipids with inositol phosphate-containing head groups. Adv. Lipid Res. **26:**253–274.
39. **Lisanti, M., I. P. Caras, M. A. Davitz, and E. Rodriguez-Boulan.** 1989. A glycophospholipid membrane anchor acts as an apical targeting signal in polarized epithelial cells. J. Cell Biol. **109:**2145–2156.
40. **Mayor, S., and H. Riezman.** 2004. Sorting GPI-anchored proteins. Nat. Rev. Mol. Cell Biol. **5:**110–120.
41. **McDowell, M. A., D. A. Ransom, and J. D. Bangs.** 1998. Glycosyl phosphatidylinositol-dependent secretory transport in *Trypanosoma brucei*. Biochem. J. **335:**681–689.
42. **Menon, A. K., S. Mayor, M. A. J. Ferguson, M. Duszenko, and G. A. M. Cross.** 1988. Candidate glycophospholipid precursor for the glycosylphosphatidylinositol membrane anchor of *Trypanosoma brucei* variant surface glycoprotein. J. Biol. Chem. **263:**1970–1977.
43. **Merrill, A. H., Jr., and K. Sandhoff.** 2002. Sphingolipids: metabolism and cell signaling, p. 373–407. *In* D. E. Vance and J. E. Vance (ed.), Biochemistry of lipids, lipoproteins and membranes, 4th ed. Elsevier, Boston, MA.
44. **Miyake, Y., Y. Kozutsumi, S. Nakamura, T. Fujita, and T. Kawasaki.** 1995. Serine palmitoyltransferase is the primary target of a sphingosine-like immunosuppressant, ISP-1/myriocin. Biochem. Biophys. Res. Commun. **211:**396–403.
45. **Muñiz, M., P. Morsomme, and H. Reizman.** 2001. Protein sorting upon exit from the endoplasmic reticulum. Cell **104:**313–320.
46. **Nolan, D. P., G. Geuskens, and E. Pays.** 1999. *N*-linked glycans containing linear poly-*N*-acetyllactosamine as sorting signals in endocytosis in *Trypanosoma brucei*. Curr. Biol. **9:**1169–1172.
47. **Nolan, D. P., D. G. Jackson, M. J. Biggs, E. D. Brabazon, A. Pays, F. Van Laethem, F. Paturiaux-Hanocq, J. Elliot, H. P. Voorheis, and E. Pays.** 2000. Characterization of a novel alanine-rich protein located in surface microdomains in *Trypanosoma brucei*. J. Biol. Chem. **275:**4072–4080.
48. **Overath, P., J. Czichos, and C. Hass.** 1986. The effect of citrate/*cis*-aconitate on oxidative metabolism during transformation of *Trypanosoma brucei*. Eur. J. Biochem. **160:**175–182.
49. **Patnaik, P. K., M. C. Field, A. K. Menon, G. A. M. Cross, M. C. Yee, and P. Butikofer.** 1993. Molecular species analysis of phospholipids from *Trypanosoma brucei* bloodstream and procyclic forms. Mol. Biochem. Parasitol. **58:**97–106.
50. **Perry, D. K.** 2002. Serine palmitoyltransferase: role in apoptotic de novo ceramide synthesis and other stress responses. Biochim. Biophys. Acta **1585:**146–152.
51. **Pinto, W. J., B. Srinivasan, S. Shepherd, A. Schmidt, R. C. Dickson, and R. L. Lester.** 1992. Sphingolipid long-chain-base auxotrophs of *Saccharomyces cerevisiae*: genetics, physiology, and a method for their selection. J. Bacteriol. **174:**2565–2574.
52. **Ralton, J. E., K. A. Mullin, and M. J. McConville.** 2002. Intracellular trafficking of glycosylphosphatidylinositol (GPI)-anchored proteins and free GPIs in *Leishmania mexicana*. Biochem. J. **363:**365–375.
53. **Rifkin, M. R., C. A. Strobos, and A. H. Fairlamb.** 1995. Specificity of etha-

nolamine transport and its further metabolism in *Trypanosoma brucei*. J. Biol. Chem. **270:**16160–16166.
54. **Salto, M. L., L. E. Bertello, M. Vieira, R. Docampo, S. N. J. Moreno, and R. M. de Lederkremer.** 2003. Formation and remodeling of inositolphosphoceramide during differentiation of *Trypanosoma cruzi* from trypomastigote to amastigote. Eukaryot. Cell **2:**756–768.
55. **Schuck, S., and K. Simons.** 2006. Controversy fuels trafficking of GPI-anchored proteins. J. Cell Biol. **172:**963–965.
56. **Schuck, S., and K. Simons.** 2004. Polarized sorting in epithelial cells: raft clustering and the biogenesis of the apical membrane. J. Cell Sci. **117:**5955–5964.
57. **Simons, K., and E. Ikonen.** 1997. Functional rafts in cell membranes. Nature **387:**569–572.
58. **Sonda, S., G. Sala, R. Ghidoni, A. Hemphill, and J. Pieters.** 2005. Inhibitory effect of aureobasidin A on *Toxoplasma gondii*. Antimicrob. Agents Chemother. **49:**1794–1801.
59. **Sutterlin, C., T. Doering, F. Schimmoller, S. Schroder, and H. Riezman.** 1997. Specific requirements for the ER to Golgi transport of GPI-anchored proteins in yeast. J. Cell Sci. **110:**2703–2714.
60. **Triggs, V. P., and J. D. Bangs.** 2003. Glycosylphosphatidylinositol-dependent protein trafficking in bloodstream stage *Trypanosoma brucei*. Eukaryot. Cell **2:**76–83.
61. **Uemura, A., S. Watarai, Y. Kushi, T. Kasma, Y. Ohnishi, and H. Kodama.** 2006. Analysis of neutral glycosphingolipids from *Trypanosoma brucei*. Vet. Parasitol. **140:**264–272.
62. **Vainauskas, S., Y. Maeda, H. Kurniawan, T. Kinoshita, and A. K. Menon.** 2002. Structural requirements for the recruitment of Gaa1 into a functional glycosylphosphatidylinositol transamidase complex. J. Biol. Chem. **277:**30535–30542.
63. **Vainauskas, S., and A. K. Menon.** 2004. A conserved proline in the last transmembrane segment of Gaa1 is required for glycosylphosphatidylinositol (GPI) recognition by GPI transamidase. J. Biol. Chem. **279:**6540–6545.
64. **van Meer, G., and Q. Lisman.** 2002. Sphingolipid transport: rafts and translocators. J. Biol. Chem. **277:**25855–25858.
65. **Zanolari, B., S. Friant, K. Funato, C. Sutterlin, B. J. Stevenson, and H. J. Riezman.** 2000. Sphingoid base synthesis requirement for endocytosis in *Saccharomyces cerevisiae*. EMBO J. **19:**2824–2833.
66. **Zhang, K., F. F. Hsu, D. A. Scott, R. Docampo, J. Turk, and S. M. Beverley.** 2005. *Leishmania* salvage and remodelling of host sphingolipids in amastigote survival and acidocalcisome biogenesis. Mol. Microbiol. **55:**1566–1578.
67. **Zhang, K., J. M. Pompey, F.-F. Hsu, J. Turk, and S. M. Beverley.** 2007. Redirection of sphingolipid metabolism towards de novo synthesis of ethanolamine in *Leishmania.* EMBO J. doi:10.1038/sj.emboj.7601565.
68. **Zhang, K., M. Showalter, J. Revollo, F.-F. Hsu, J. Turk, and S. M. Beverley.** 2003. Sphingolipids are essential for differentiation but not growth in *Leishmania*. EMBO J. **22:**6016–6026.